Directional Diffusion Anti-Aliasing (DDAA)

Almar Klein
Independent scholar

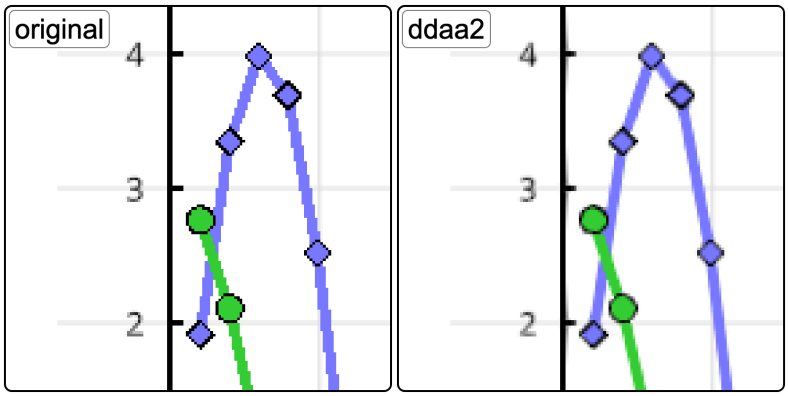

Figure 1. Result of applying DDAA to an example image.

Abstract

Post-processing Anti-Aliasing (PPAA) is a widely used technique for real time rendering. Its benefits include simplicity and performance, and because it applies anti-aliasing to the full rendered image, it is also useful in cases where MSAA cannot be used, such as for lines, markers, and text rendering.

The proposed method builds on two existing categories of PPAA techniques. Firstly, the direction of an edge is estimated and then diffused along the edge, thereby softening the edge's appearance without blurring it. Secondly, an edge-search walks horizontally or vertically along the gradient direction, computing a subpixel offset to produce a smooth gradient in long edges. The algorithm improves on the aforementioned techniques by a more accurate edge-angle measurement, maintaining small structures, and avoiding artifacts by performing a complete edge search.

Quantitative and qualitative evaluation show that DDAA produces better results, making it a suitable alternative, especially for scientific visualizations such as plots. Furthermore, it introduces optimizations that allow it to outperform FXAA.

 ISSN 2331-7418

1. Introduction

1.1. Strategies for anti-aliasing

The most effective way to reduce aliasing effects in rendered images is Super-Sample Anti-Aliasing (SSAA), in which the image is rendered at a higher resolution than the final resolution, and then downsampled with an appropriate filter. However, in real-time rendering, the larger number of pixels impacts fragment shader performance, as well as memory usage. This makes SSAA with large sampling factors impractical, while smaller factors (e.g. $<= 2$) are less effective at countering aliasing.

The Multi-Sample Anti-Aliasing (MSAA) method addresses the performance problem by storing multiple samples at mesh edges, without significantly increasing fragment shader cost. It is a widely used technique in video games, but because it does not address aliasing effects for fragments that are *not* on the edge of a mesh, it is not generally applicable. Examples for which MSAA does not help include rendering of thick lines, markers, grids, sdf-based text, etc. Therefore, MSAA is barely useful in scientific applications.

For the aforementioned lines, markers, and text it is common practice to implement anti-aliasing in the fragment shader by reducing the fragment's alpha value at the edge of the object, e.g. [Rougier 2014]. This can be an effective method, since the coverage of the current fragment can usually be calculated. However, if such an object was originally opaque, it will now result in a mix of opaque and semi-transparent fragments, which is problematic because renderers typically treat such fragments differently. E.g. transparent objects must typically be ordered from back to front to be rendered correctly. Therefore, this approach is prone to artifacts, especially in 3D scenes [Klein 2025].

With Temporal Anti-Aliasing (TAA), multiple successive frames are considered to reduce aliasing in both the spatial and temporal dimensions [Yang et al. 2020; Karis 2014]. This technique has gained popularity in modern games, but is also known to suffer from typical artifacts such as ghosting and smearing. Furthermore, this technique assumes a steady stream of images, which is not always the case for scientific visualizations. Sometimes there is just one frame, or new frames may only be rendered when the scene has changed. For these reasons, the current study focuses on methods that only operate on the current frame.

Post-Processing Anti-Aliasing (PPAA) algorithms attempt to reduce the aliasing effects on the image after it has been rendered, by subtly changing the values of individual pixels, mostly at edges/boundaries in the image. Because it is applied as a post-processing step, it is relatively easy to implement, without affecting the rendering pipelines or shaders, and is usually more performant than MSAA and SSAA. However, PPAA is applied once the aliasing has already occurred, so artifacts can not always be *removed*, but rather their appearance can be *softened*. Similarly, while

Name	Algorithm summary
blur	Simple blurring using a 3x3 kernel with (truncated) Gaussian weights.
ssaax2	Super-Sample Anti-Aliasing with a factor 2 (4 times as many pixels).
ssaax4	Super-Sample Anti-Aliasing with a factor 4 (8 times as many pixels).
fxaa3c	Fast-Approximate Anti-Aliasing 3.11 console version (no edge-search).
fxaa3d	Fast-Approximate Anti-Aliasing 3.11 desktop version (with edge-search).
ddaa1	The proposed algorithm version 1.1 (no edge-search).
ddaa2	The proposed algorithm version 2.4 (with edge-search).

Table 1. Overview of the of the different algorithms compared in this paper. Unless stated otherwise, the term "FXAA" means `fxaa3d`, and "DDAA" means `ddaa2`.

individual frames can look good, a stream of images can have temporal artifacts as boundaries shift from one pixel to another.

In the present work, a novel PPAA algorithm is presented, with several benefits compared to existing methods.

1.2. Post-processing anti-aliasing

The many known PPAA algorithms can be roughly divided into three categories.

In morphological anti-aliasing, structures in the image are identified and subpixel blending is applied depending on the detected shape. Examples are MLAA [Reshetov 2009], SMAA [Jimenez et al. 2012] and CMAA [Davies 2014].

Another common approach is to estimate the direction of the edge, and apply some kind of blurring along the edge, but not perpendicular to it, so that the edge remains sharp. Examples include early versions of FXAA and the console versions of FXAA 3.11 [Lottes 2009], as well as some lesser known algorithms such as Directionally-Localized Anti-Aliasing [ForserX 2022].

The "desktop" version of FXAA 3.11 [Lottes 2009], can be considered a different category, as it walks vertically or horizontally along the gradient direction, sampling outward in both directions until the local contrast falls below a threshold, then using the measured span to compute a subpixel offset so that the final sampled pixel corresponds with the reconstructed edge. The variable number of texture lookups results in some loss of performance, but it results in smooth transitions for edges that are nearly horizontal/vertical, as shown in Figure 2. Improvements to this algorithm have also been proposed, e.g. adaptive approximate anti-aliasing (AXAA) [Nah et al. 2016].

Table 1 lists the different algorithms that are compared in the current work. For comparison, this work also includes a method that simply blurs the image with a truncated Gaussian kernel.

Figure 2. Comparison of different algorithms on an image containing multiple near-horizontal and near-vertical edges. The algorithms that include edge-search (`fxaa3d` and `ddaa2`) produce a notably smoother result.

2. Proposed algorithm

The proposed algorithm, Directional-Diffusion Anti-Aliasing (DDAA) consists of multiple contributions: an improved method to estimate the angle of edges for consistent diffusion, the combination of directional diffusion and edge-search, a cleaner edge-search without artifacts, and batched sampling during edge-search. These contributions are discussed in detail in the following subsections.

For the proposed algorithm, we distinguish between a simpler version without edge-search (`ddaa1`), and the full version with edge-search (`ddaa2`).

2.1. Directional diffusion

The first contribution—after which the algorithm is named—is the way that the direction of the edge is measured and how the subsequent diffusion (i.e. smoothing) is performed.

To measure the direction of an edge, different kernels can be used. A commonly used derivative kernel is the Sobel operator. However, it has been shown that this filter is not directionally invariant, and better kernels exist [Jähne et al. 1999; Kroon 2009].

We performed an experiment, applying different kernels to estimate the angle of an edge in an image containing a line at a known angle. We then compared the measured angles with the reference angle to calculate the error. The results in Figure 3 illustrate that the Scharr kernel [Jähne et al. 1999] performs much better than the Sobel operator. Errors in the measured angles result in excessive and angle-dependent blurring, as shown in the `fxaa3c` panel in Figure 4. For this reason, the proposed algorithm uses the Scharr kernel, resulting in a consistent smoothing, see the `ddaa1`

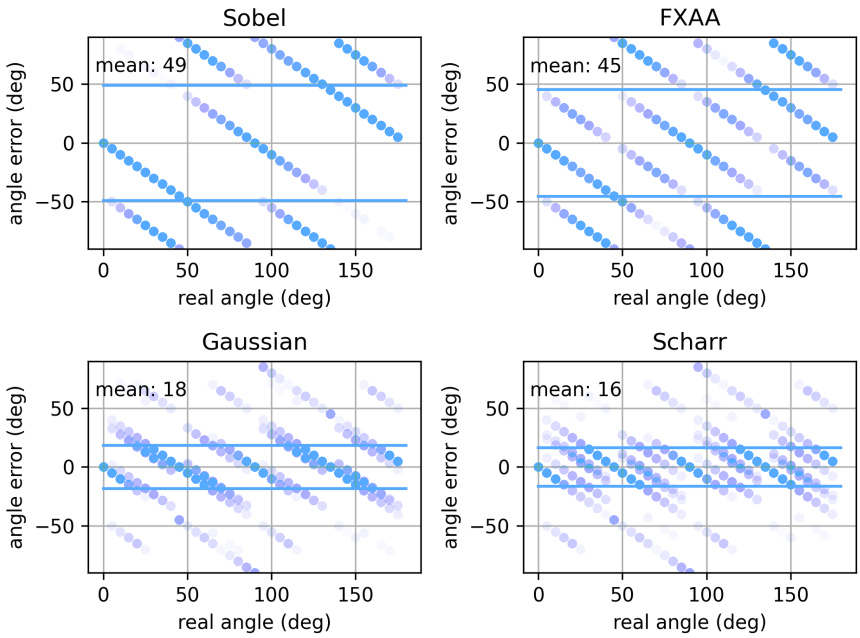

Figure 3. Comparison of angle estimation errors for different kernels. The mean error in degrees are shown in the plots using the horizontal lines and its value in text. The Scharr kernel is most capable of estimating an edge's angle.

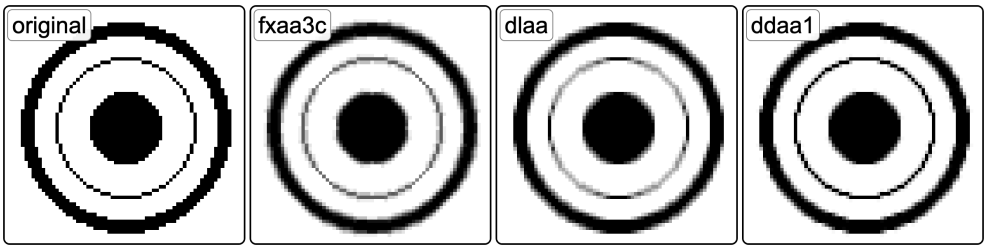

Figure 4. Comparison of PPAA algorithms that estimate the angle of an edge and then smooth in its direction. Errors in the estimate of the edge's angle result in an uneven and blurry appearance of the circles. Due to its improved angle estimate, DDAA produces the most uniform result.

panel in Figure 4.

To perform diffusion (i.e. smoothing) in a particular direction, an elongated kernel should be used. In practice, two (bilinearly interpolated) samples are taken that lie on a line. A larger distance between the samples results in more diffusion, The maximum distance from the center is such that the contribution of the center pixel is the largest, and that the contribution of neighboring pixels does not lead to excessive blurring. See Figure 5.

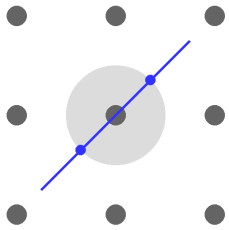

Figure 5. Illustration of the directional diffusion of a single pixel. Exactly 2 samples are taken, on opposite sides from the center pixel, and no further than 0.5 pixel distance from the center, i.e. inside the large gray circle. The blue line and dots indicate a maximum diagonal diffusion. Using a larger distance, such as $\sqrt{2}$, would for diagonal lines put each sample right in between 4 pixels, which would result in an overly blurry result.

```
diffuseStrength = calculateDiffuseStrength()
subpixelEdgeOffset = calculateSubpixelOffset()

edgeStrength = length(2.0 * subpixelEdgeOffset)
diffuseStep = diffuseDir * diffuseStrength * (1.0 - edgeStrength)

texCoord1 = texCoord - diffuseStep + subpixelEdgeOffset
texCoord2 = texCoord + diffuseStep + subpixelEdgeOffset
```

Listing 1. Pseudo-code to combine diffusion with edge-search. The real code can be found at https://github.com/almarklein/ppaa-experiments/blob/main/wgsl/ddaa2.wgsl.

2.2. Combining diffusion with edge-search

The diffusion discussed in the previous subsection provides good results, except for lines that are nearly horizontal or vertical. In such cases, the amount of diffusion required to provide a smooth result is enormous and prone to artifacts.

Handling such ”long edges” is a key contribution of FXAA (desktop version); the proposed algorithm adopts a similar edge-search strategy. The idea is to determine how far the current pixel is to the nearest end of the line segment, and then sample the current pixel with a small subpixel offset perpendicular to the edge, where the offset is determined by the distance to the end.

In effect, the proposed algorithm employs two types of blurring: the diffusion in the direction of the edge, and the subpixel offset from the edge-search. These are combined by a) applying the offset to both samples mentioned in section 2.1 and shown in Figure 5; b) diminishing the diffusion strength based on the magnitude of the subpixel offset. This results in a smooth transition as an edge goes from horizontal to diagonal, to vertical. See Listing 1 for details.

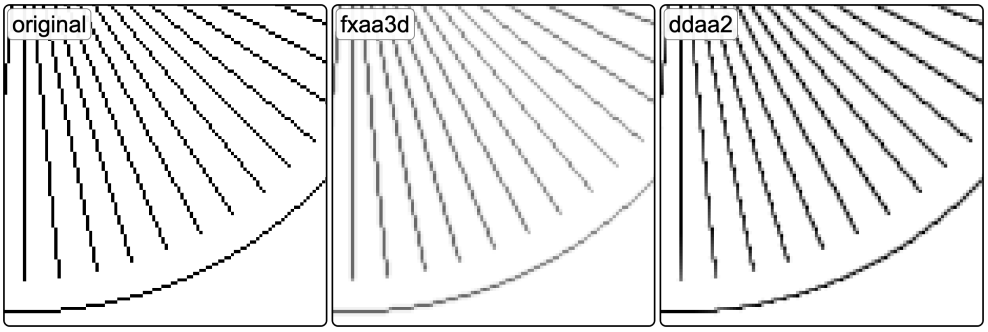

Figure 6. Comparison of FXAA and DDAA on an image containing thin lines. With FXAA the line is less visible, while DDAA maintains the line.

2.3. Preserving small structures

FXAA is known to diminish small structures. An approach to prevent this has been proposed as part of AXAA [Nah et al. 2016]. The idea is to detect when a pixel is on a ridge, and then disable any blurring. However, the implementation in AXAA only does this for positive ridges, not for valleys. In the proposed algorithm, both ridges and valleys are considered.

Further, the amount of diffusion is diminished depending on the steepness of the ridge/valley, instead of an on/off approach based on a threshold. The effect comparing FXAA and DDAA is illustrated in Figure 6.

2.4. Clean edge-search

During the edge-search, which is implemented in both FXAA (`fxaa3d`) and DDAA (`ddaa2`), the algorithm walks vertically or horizontally along the edge, sampling outward in both directions until the end of the edge is detected.

Since it is now known beforehand how many samples are required, the algorithm adopts a maximum distance to search in. Searching further produces smoother transitions in the end-result, at the cost of performance. Multiple strategies can be applied to improve the performance or distance of the edge-search.

The FXAA algorithm uses a strategy that increases the size of the steps it takes along the edge, effectively skipping pixels; it starts with steps of 1 pixel, but increases the step size to 2, 4 and even 8 pixels. The idea is that if the edge was already found to be quite long, there's a good chance it is even longer. By skipping pixels, the algorithm can search much further along the edge without losing too much performance. Many derived algorithms, including [Nah et al. 2016] use a similar strategy in their edge-search.

The downside is that the algorithm can miss the end of the ridge, which leads to stipply artifacts. In natural images such cases are rare and the artifacts usually not severe. However in artificial data, e.g. in scientific plots, such cases are much more

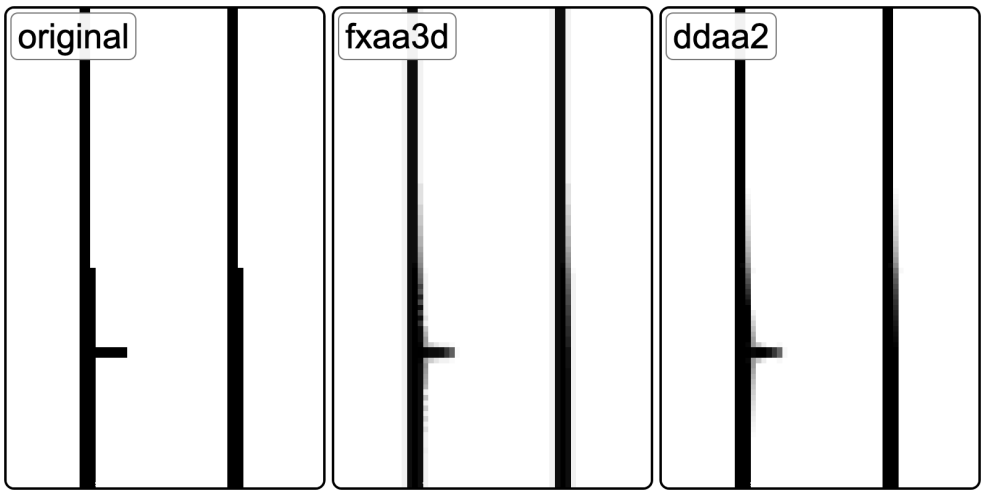

Figure 7. Comparison of FXAA and DDAA on an image that contains two near-vertical lines, one of which has an obstruction to "end the edge". FXAA introduces artifacts because it skips pixels (i.e. misses the obstruction), while DDAA produces a clean albeit slightly shorter gradient.

likely to occur and the artifacts also more pronounced due to the high contrast.

In Figure 7 the effect can be observed. It also shows how DDAA does not suffer from these artifacts; it consistently takes steps of 1 pixel, without skipping any.

While this strategy fixes this particular group of artifacts, it is also more costly. To compensate for that, DDAA uses a trick to take samples more efficiently, which is explained in the next section. Further, DDAA's edge-search is less long than that of FXAA; With the default configuration FXAA takes 12 samples, reaching 26 pixels. The default configuration of `ddaa2` reaches 15 pixels.

2.5. Batched sampling in edge-search

The proposed algorithm makes use of the WGSL function `textureSampleLevel()` with the integer offset parameter, which must be in the range $[-8..7]$. The edge-search takes multiple samples at each step, using the same texture coordinate, but with different integer offsets.

This *batched sampling* allows the GPU compiler to do multiple texture fetches in parallel, thereby saving time, and improving the overall performance of the algorithm.

One important parameter is the number of samples per batch. The number of fetches that can run in parallel is limited, and with larger numbers the algorithm is increasingly likely to take more samples than needed. A good value for the number of samples per batch was determined empirically, using the same hardware as in Section 3.4. The details of these experiments are out of scope for the current paper, but they suggested that a value of 3 is appropriate. See Listing 2 for an example.

```
v1 = textureSampleLevel(tex, smp, currentUv, 0.0, vec2i(-1, 0)).rgb;
v2 = textureSampleLevel(tex, smp, currentUv, 0.0, vec2i( 0, 0)).rgb;
v3 = textureSampleLevel(tex, smp, currentUv, 0.0, vec2i( 1, 0)).rgb;
```

Listing 2. Pseudo-code to take 3 horizontal samples in a way that allows the compiler to optimize. The real code can be found at https://github.com/almarklein/ppaa-experiments/blob/main/wgsl/ddaa2.wgsl.

It is worth mentioning that FXAA does not include this optimization because sampling with an integer offset was not yet available at the time.

Another small optimization is possible by calculating the first edge-search sample from the luma values that are already known, thus saving two texture-fetches (one for each direction).

3. Evaluation

The following subsections describe the experiments that were performed to evaluates the proposed algorithm in terms of quantitative errors, qualitative comparisons, temporal effects, and performance. All tests were based on the four test images shown in Figure 8.

3.1. Quantitative errors

3.1.1. Methods

In order to quantify the quality of the algorithms considered in this study, we compared the result of each method to a reference image.

The most straightforward approach would be to compare the images directly to the result of e.g. an 8x SSAA method. However, it was found that this approach tends to favor blurry images, making the quantized errors ineffective for representing the quality of the PPAA methods.

Therefore, we upscaled each image (obtained by the different PPAA methods) to 8 times the resolution, using a cubic Mitchel filter, so it was the same size as the reference image (which was generated at 8 times the normal resolution). Next, the peak signal-to-noise ratio (PSNR) was calculated from the image and the reference. The resulting values thus indicate how closely each image can be reconstructed relative to the reference image.

Since there still appears to be a preference for blurry images, the 'blur' method was included for comparison, which performed a Gaussian blur with sigma 0.6.

3.1.2. Results

The results are shown in Table 2. The numbers are all close together, but it can be observed how `ssaax4` and `ssaax2` consistently perform the best, while the `blur`

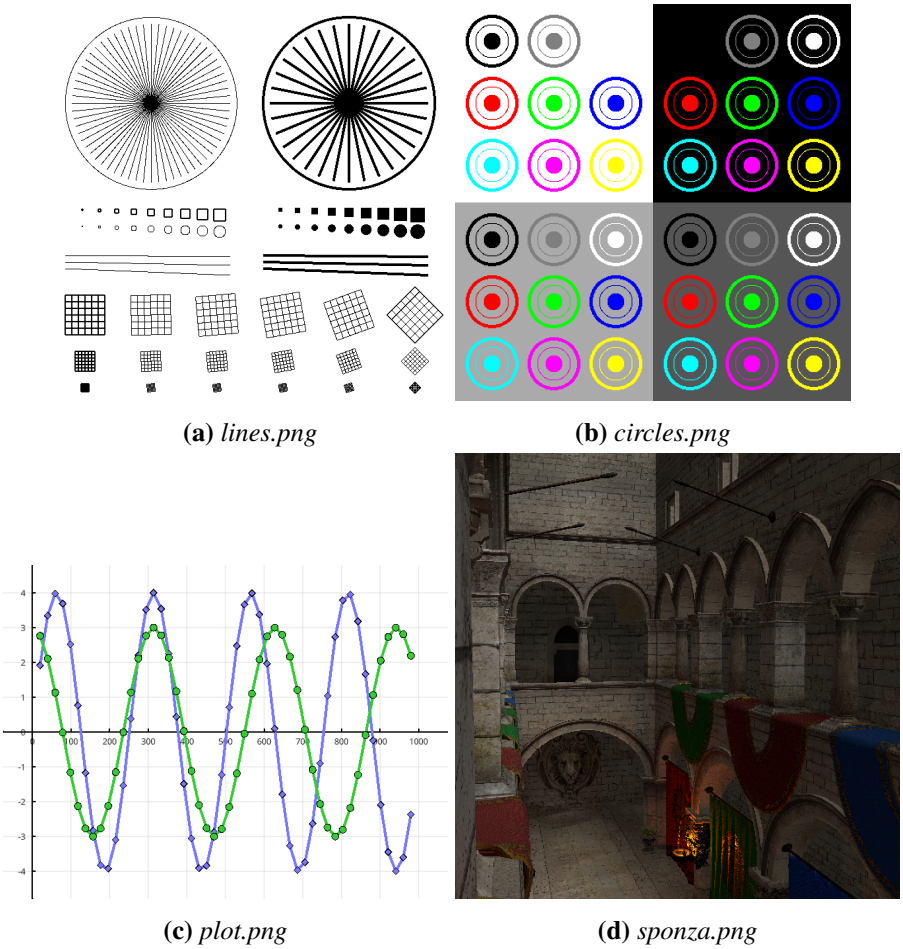

(a) *lines.png* **(b)** *circles.png*

(c) *plot.png* **(d)** *sponza.png*

Figure 8. The four test images used for visual comparison and benchmarking.

Image	ssaax4	ssaax2	blur	fxaa3c	fxaa3d	ddaa1	ddaa2
lines	17.3	17.2	16.2	16.2	16.0	17.1	16.9
circles	22.5	22.4	21.3	21.6	21.8	22.3	22.2
plot	23.6	23.5	22.4	22.7	22.7	23.7	23.2
sponza	30.2	30.0	29.2	29.1	29.2	29.2	29.2
total	23.4	23.3	22.3	22.4	22.4	23.1	22.9

Table 2. The peak signal-to-noise ratio for the different PPAA methods (dB).

method acts as a baseline for a ”poor” result.

The `fxaa` methods barely outperforms the `blur` method; although they are less blurry, they also introduce more artifacts. The `ddaa` methods produces significantly better results, especially for the ’line’ and ’plot’ images.

Interestingly, the `ddaa1` method outperforms `ddaa2` on most images. It appears

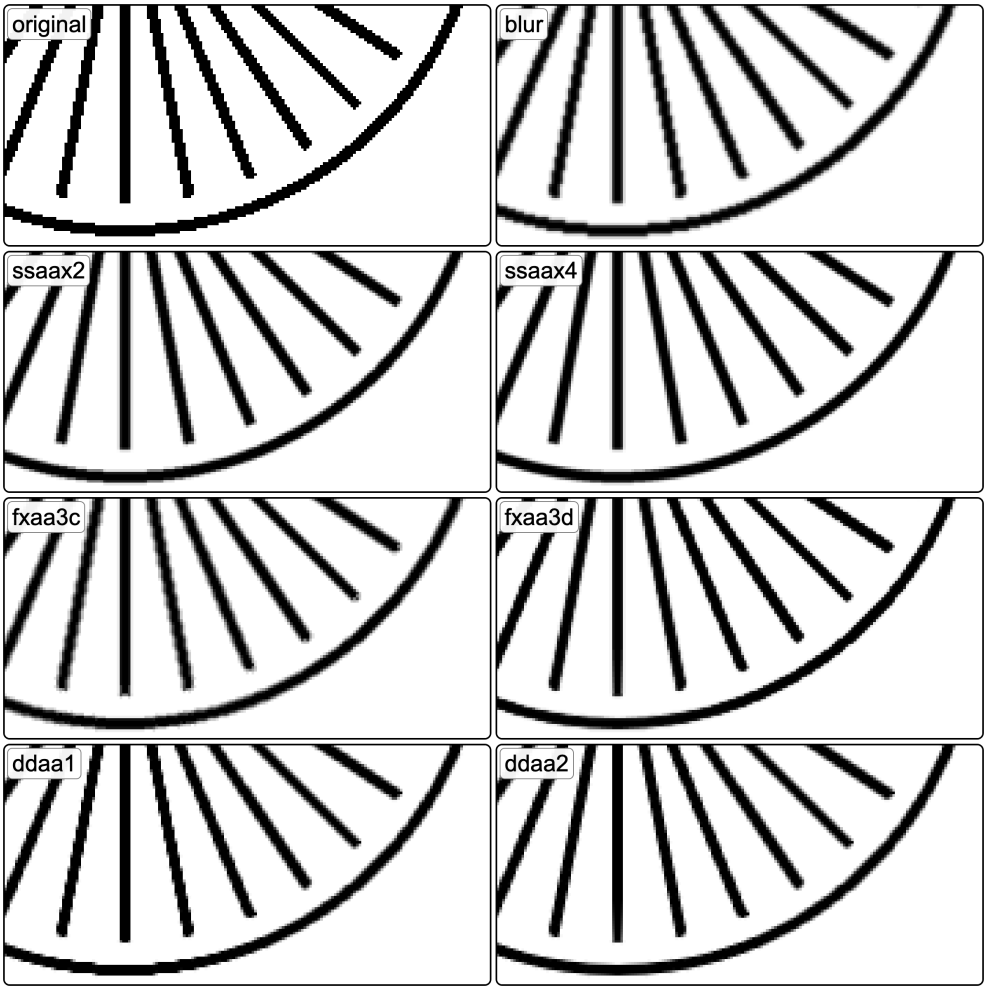

Figure 9. Comparison of all considered PPAA algorithms on an image containing lines at different angles. It can be seen that `ddaa2` produces the most consistent smoothness for different angles.

that these measurements do not capture the advantages of the edge search performed in `fxaa3d` and `ddaa2`; to evaluate the proposed algorithm, we also need thorough qualitative comparisons.

3.2. Qualitative comparisons

3.2.1. Methods

The goal of a PPAA algorithm is to reduce the effects of aliasing so the image is pleasing to the eye. To investigate whether this is successful, a selection of negative effects that should be reduced and/or avoided are listed. The visual results are then compared against this list.

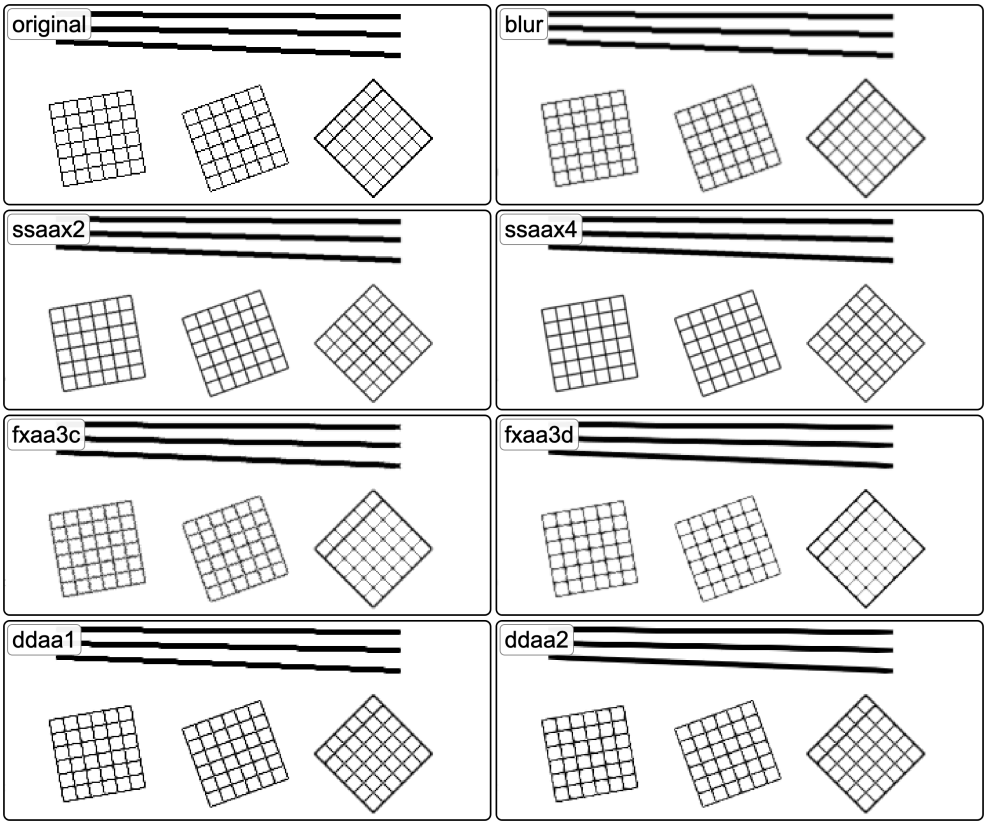

Figure 10. Comparison of all considered PPAA algorithms on an image containing near-horizontal lines and a few grids. It can be seen that `fxaa3d` and `ddaa2` produce a smoother edge because of the edge-search. The grids look clean for `ddaa2` while `fxaa3d` show artifacts.

- Jagged structures (mostly apparent in near-diagonal lines).
- Steps in straight lines (mostly apparent in near-horizontal or vertical lines).
- Excessive smoothing (can be introduced by the algorithm).
- Other artifacts (can be introduced by the algorithm).

3.2.2. Results

In Figure 9 the proposed algorithm (`ddaa2`) is compared against other algorithms. It can be observed that the diagonal lines are less jagged than they are for `fxaa3d`, but also not blurry like `fxaa3c`. It can also be seen that near-vertical and near-horizontal lines are smooth, albeit the length of the 'gradient' is slightly shorter than that of `fxaa3d`.

In Figure 10, the algorithms that perform edge-search (`fxaa3d` and `ddaa2`) the near-horizontal edge is smoothed by a gradient. The gradient for `fxaa3d` is some-

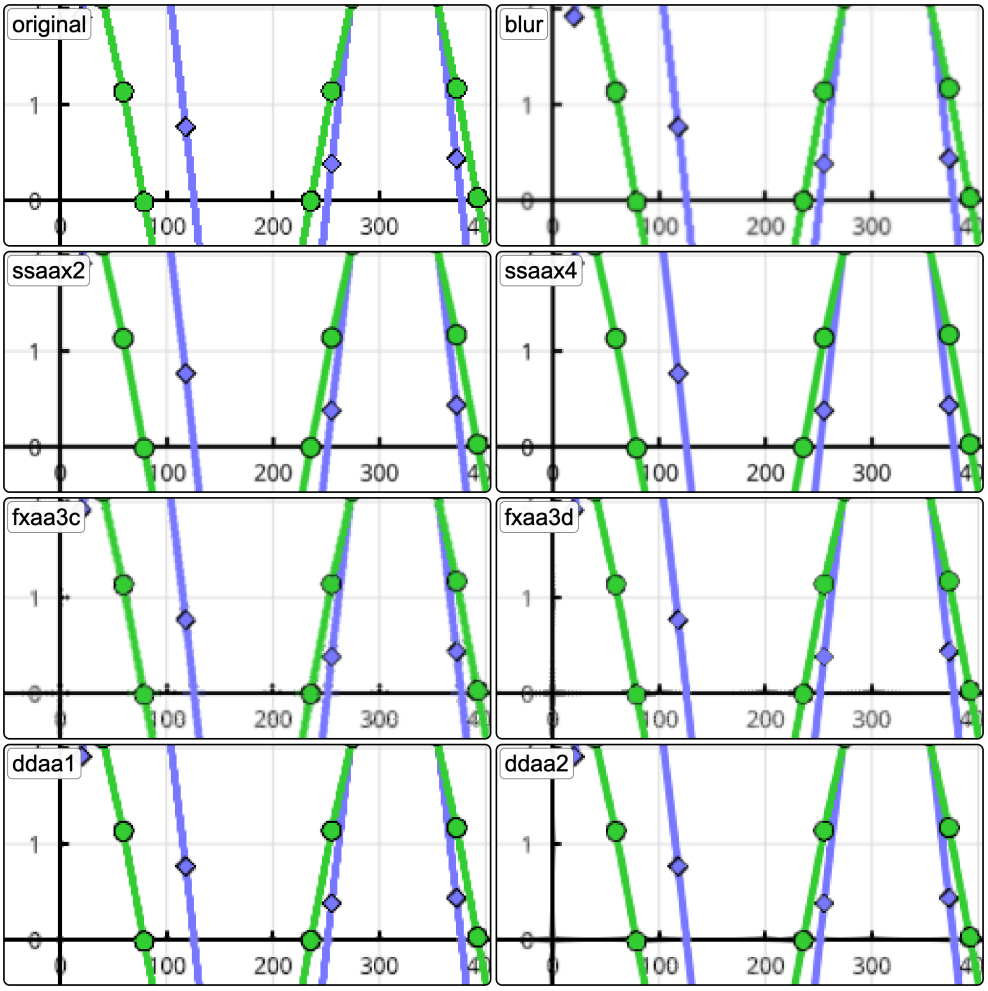

Figure 11. Comparison of all considered PPAA algorithms on an image depicting a plot. It can be seen that `dddaa2` shows clean text, crisp circles, and does not have the dotted artifacts that the `fxaa` algorithms suffer from because they skip pixels.

what longer, but shows steps. This illustrates how the proposed algorithm exchanges a bit of edge-search distance for correctness. The same image also shows a fine grid, that has artifacts for the `fxaa` algorithms. The `ddaa` algorithms don't have these artifacts because they preserve small structures.

In Figure 12, a piece of the plot image is shown. The `fxaa` algorithms perform paticularly poor, demonstrating hard to read text, marker edges that are badly visible at certain angles, and stipple artifacts around tick marks. The `ddaa` algorithms looks better on all these aspects.

In Figure **??**, a few coloured circles are depicted. The figure shows that going around a circle, the `ddaa2` method has the most uniform amount of blur. It also looks closest to the `ssaax4` (which can be considered a reference). In contrast `fxaa3c` is

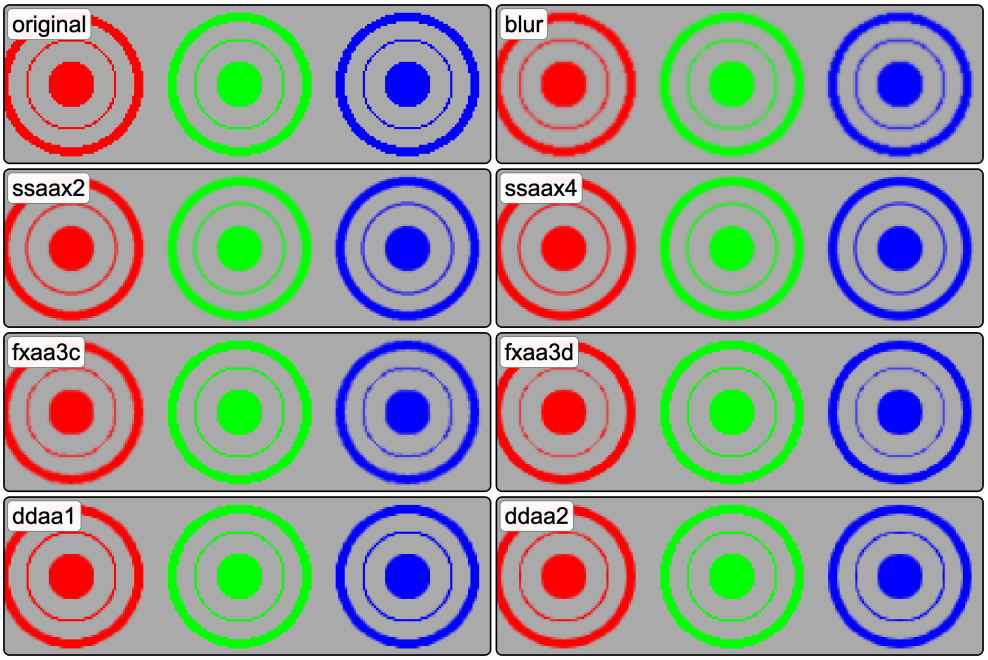

Figure 12. Comparison of all considered PPAA algorithms on an image depicting circles. It can be seen that the `ddaa2` method has the most uniform diffusion (independent ot the angle of the line), that thin lines are not diminished.

more similar to the `blur` method and `fxaa3d` diminishes thin lines. It can be seen that the green circle not smoothed by any of the PPAA methods. This is because these methods convert RGB colors to a scalar luma value, and the luma of certain colors is so close to the luma of the background, that the contrast falls below the algorithms threshold. This is an intrisic limitation of most PPAA methods, which is not easy to overcome due to limited availability of registers in a shader program.

3.3. Temporal effects

The current work is constrained to PPAA methods that operate on a single frame (i.e. excluding algorithms that use multiple successive frames), because it covers use-cases where only a single frame is available, or where there is not much motion, such as in scientific visualizations. Nevertheless, it's valuable to evauluate the results in use-cases where animations and motions are present.

3.3.1. Methods

We created an animated image, which can be seen (in static form) in Figure 13. The image consists of 32 frames that form a loop, which is played at about 25 FPS, stored in an animated PNG file

All considered algorithms are applied to each frame separately, after which the

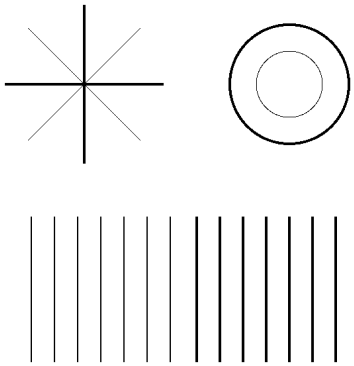

Figure 13. The image used to study temporal effects. The actual image is an animated png: the top-left cross rotates around it's center, the top-right circles rotate around an off-center point, and the vertical lines slant back and forth. See https://almarklein.github.io/ppaa-experiments/viewer.html#image=animated.png for the animated version.

processed frames are saved in a new animated PNG file.

The animations can visually compared in the available viewer application, where one can zoom in on certain regions to study the differences.

3.3.2. Results

The slanting lines demonstrate the clearest temporal artifacts, with visual 'jumps' occuring as the part of a line moves to the neighbouring pixel, also known as 'shimmering' or 'jitter'.

As expected, the `ssaa` methods show a smaller (more fine-grained) jump. In the methods that apply edge-search, the jump is still visible, because the jump is present in the source image and the algorithm does not have access to information regarding the motion. However, the jump does appear smoother because it's 'smeared out' over a large (vertical) region.

The `fxaa` methods show a clear shimmering effect for the thin-lined cross and the thin (inner) circle. This can be attributed to the inconsistent smoothing. In the `ddaa` methods, with their improved angle measurement, this effect is much less prominent.

3.4. Performance

3.4.1. Methods

To measure the performance in terms of speed, we performed benchmarks on a range of different hardware, including integrated GPUs, Apple Silicon GPUs, and dedicated GPUs.

The render-pass for each algorithm was run 100 times, while the time spent by the GPU was measured using a timestamp query. The mean and standard deviations were

Device	blur	ssaax2	fxaa3c	ddaa1	fxaa3d	ddaa2
Intel UHD 630	100	74	94	98	230	175
Intel UHD 730	100	72	84	125	352	247
AMD Radeon 780M	100	87	81	94	186	184
MacBook M1 Pro	100	94	95	104	219	197
Nvidia RTX 2070	100	71	105	139	282	255
Nvidia RTX 3050	100	80	98	125	160	180
Nvidia RTX 5060 Ti	100	82	102	150	202	203

Table 3. The performance of the considered PPAA algorithms. The values represent relative performance (% of `blur` baseline). Lower values indicate faster performance.

displayed. A high standard deviation indicates that the GPU was likely also doing other work, so the benchmark could be repeated.

To make it easier to compare the numbers across devices, the measured times were normalized by using the time for the ”blur” algorithm as a reference. (Since its speed is in the same order of magnitude as the PPAA methods, using the blur shader as a reference yields more stable numbers than a shader that only copies the image.) The final result was calculated by taking the mean of the four test images shown in Figure 8.

3.4.2. Results

The final results are shown in Table 3. The values for `blur` are all 100%, since it is used as the baseline.

The `ssaax2` shader is not a PPAA algorithm, but included for comparison. This shader is a cubic Mitchel filter, optimized to take just 12 texture samples. It performs consistently faster than the blur filter, which is surprising because the latter takes only 9 texture samples. This illustrates that SSAA with a factor 2 is a feasible method. Note that the costs for rendering the frame at a higher resolution are not included in the benchmarks, but these costs would be the same as when a HiDPI screen would have been used.

The `ssaax4` shader is not included in the benchmarks because it is not as highly optimized in the implementation, and requires 64 texture samples.

As expected, the simpler algorithms `fxaa3c` and `ddaa1` are faster than the algorithms that apply an edge-search. They can be faster than the blur filter because of the early exit strategy for low-contrast regions. The `ddaa1` algorithm is consistently slightly slower than `fxaa3c`.

In Intel integrated graphics and Apple Silicon, DDAA performs consistently better than FXAA. This suggests that the optimization of batching samples is helping the hardware run the algorithm faster. For AMD integrated graphics, DDAA and FXAA have similar performance.

For the dedicated graphics cards (all Nvidia), DDAA performs either better or similar to FXAA, depending on the model.

4. Discussion and recommendations

The previous section shows that the proposed algorithm `ddaa2` is a suitable alternative for existing PPAA methods, especially on scientific images. The edge-search produces better results for certain artifacts than `ssaax2`.

Although it is capable of softening temporal artifacts somewhat, motion artifacts can be considered it's main weakness (as for all PPAA methods).

It can be observed that on HiDPI displays (which have 2 times the physical resolution as a normal display) the temporal artifacts are much less prominent, which can be expected since the images are rendered at twice the resolution, which is similar to what happes with `ssaax2`.

This observation was the inspiration for an aproach that was adoped in the PyGfx render engine, and that can be recommended in cases where rendering at a high resolution can be afforded: if the screen is HiDPI, render to the native resolution and apply `ddaa2`. Otherwise, render to an offscreen texture that is twice the resolution, apply `ddaa2` and then render that to the native resolution using an appropriate downsample filter (e.g. Mitchell). This is effectively a combination of `ssaax2` and `ddaa2`.

With this approach, the GPU load (and performance) are more or less indpendent on the kind of screen being used, and yields a comparable level of motion artifacts.

To avoid complicating this work, this approach was not included as one of the methods compared in the experiments. But its result can be observed in the viewer application, where it is named `ddaa2p` ("p" for plus). In all images it demonstrates a suprior quality, comparable with `ssaax4`. Particularly in the animation, it can be seen that the temporal artifacts are much less prominent than the other algorithms.

In heavy workloads where FPS matters more than motion artifacts (e.g. games), it is recommended to render to native resolution (or half-resolution on HiDPI displays). Using temporal anti-aliasing methods are then preferred to aliviate motion artifacts. Although the `ddaa2` method can still be an interesting alternative, for performance, to avoid the artifacts specific to temporal methods (e.g. ghosting), or simply because the method is easy to adopt.

5. Conclusion

The proposed Directional-Diffusion Anti-Aliasing (DDAA) algorithm has multiple advantages over existing methods such as FXAA. These include fewer jagged artifacts at diagonal edges, no excessive blurring, and maintaining small features. Its edge-search has less reach but does not skip pixels, thereby avoiding artifacts.

Quantitative and qualitative experiments demonstrate that DDAA produces bet-

ter results than existing methods, and its performance is better or similar to FXAA, depending on the hardware.

Together, these features make DDAA a promising option for real-time anti-aliasing, especially for scientific visualization and other rendering domains where precision and clarity are important.

References

DAVIES, L. Conservative morphological anti-aliasing (cmaa) - march 2014 update. Technical report, Intel, 2014. URL: https://software.intel.com/en-us/articles/conservative-morphological-anti-aliasing-cmaa-update. 3

FORSERX. Dlaa: Directionally localized antialiasing. https://github.com/ForserX/DLAA, 2022. 3

JIMENEZ, J., ECHEVARRIA, J. I., SOUSA, T., AND GUTIERREZ, D. SMAA: Enhanced subpixel morphological antialiasing. *Computer Graphics Forum*, 31(2pt1):355–364, 2012. EUROGRAPHICS 2012. 3

JÄHNE, B., SCHARR, H., AND KÖRKEL, S. Principles of filter design. In *Handbook of Computer Vision and Applications*. Academic Press, 1999. 4

KARIS, B. High quality temporal supersampling. In *SIGGRAPH Courses: Advances in Real-Time Rendering in Games*, 2014. URL: https://de45xmedrsdbp.cloudfront.net/Resources/files/TemporalAA_small-59732822.pdf. Unreal Engine 4 TAA technical material. 2

KLEIN, A. The advantage of the ordered2 blend mode and how to go without it. Issue on the Pygfx repository on Github, 2025. URL: https://github.com/pygfx/pygfx/issues/1003. 2

KROON, D.-J. Numerical optimization of kernel based image derivatives. White paper, University of Twente, 2009. URL: http://www.k-zone.nl/Kroon_DerivativePaper.pdf. 4

LOTTES, T. Fxaa. White paper, NVIDIA, 2009. URL: http://developer.download.nvidia.com/assets/gamedev/files/sdk/11/FXAAWhitePaper.pdf. 3

NAH, J.-H., KI, S., LIM, Y., PARK, J., AND SHIN, C. Axaa: adaptive approximate anti-aliasing. In *ACM SIGGRAPH 2016 Posters*, SIGGRAPH '16, New York, NY, USA, 2016. Association for Computing Machinery. ISBN 9781450343718. URL: https://doi.org/10.1145/2945078.2945129. 3, 7

RESHETOV, A. Morphological antialiasing. In *Proceedings of the Conference on High Performance Graphics 2009*, pages 109–116. ACM, 2009. 3

ROUGIER, N. P. Antialiased 2d grid, marker, and arrow shaders. *Journal of Computer Graphics Techniques (JCGT)*, 3(4):1–52, November 2014. ISSN 2331-7418. URL: http://jcgt.org/published/0003/04/01/. 2

YANG, L., LIU, S., AND SALVI, M. A survey of temporal antialiasing techniques. *Computer Graphics Forum*, 39(2):607–621, July 2020. URL: https://doi.org/10.1111/cgf.14018. 2

Index of Supplemental Materials

- The DDAA algorithm is developed at https://github.com/almarklein/ppaa-experiments. This repository contains the source code, test images, and a small Python framework to run the PAA shaders.
- The shader code is available at https://github.com/almarklein/ppaa-experiments/blob/main/wgsl/ddaa2.wgsl.
- A web viewer to compare the outputs of multiple PPAA algorithms is available at https://almarklein.github.io/ppaa-experiments/viewer.html.

Author Contact Information

Almar Klein
Almar Klein Scientific Computing
De Steiger 24
1351 AB Almere, The Netherlands
(https://almarklein.org)
almar@almarklein.org

Almar Klein, Directional Diffusion Anti-Aliasing (DDAA), *Journal of Computer Graphics Techniques (JCGT)*, vol. volume, no. issue, 1–6, yyyy
http://jcgt.org/published/vol/issue/num/

Received:	yyyy-mm-dd		
Recommended:	yyyy-mm-dd	Corresponding Editor:	Editor Name
Published:	yyyy-mm-dd	Editor-in-Chief:	Eric Haines